Journal of Building Engineering 54 (2022) 104588

Contents lists available at ScienceDirect

Journal of Building Engineering

journal homepage: www.elsevier.com/locate/jobe

Acoustic properties of commercially available thermal insulators – An experimental study

Valtteri Hongisto *, Pekka Saarinen, Reijo Alakoivu, Jarkko Hakala

Turku University of Applied Sciences, Acoustics Laboratory, Joukahaisenkatu 7, FI-20520, Turku, Finland

ARTICLE INFO

Keywords:
Thermal insulators
Airborne sound insulation
Sound absorption
Dynamic stiffness
Market survey
Acoustic performance
Impact sound insulation
Flow resistivity

ABSTRACT

Thermal insulators are used structural applications, such as walls, floors, doors, roofs, duct wrappings, machine and wall linings, and vehicle envelopes. There is very little scientific comparative research about the acoustic performance of thermal insulator materials. The purpose of our study was to compare various acoustic properties of insulator materials to improve comprehensive understanding. Thirteen commercially available insulator types produced by several manufacturers were studied for thicknesses 50, 100, and 200 mm. The materials were stone wool, glass wool, cellulose, wood fiber, expanded polystyrene, polyisocyanurate, phenol foam, and cellular glass. Six acoustic quantities were measured: sound reduction index of bare insulator, sound reduction index of encapsulated insulator (insulator between two boards), sound absorption coefficient, airflow resistivity, dynamic stiffness, and reduction of impact sound pressure level in a floating floor. The acoustic performance differed significantly between insulator types for each quantity. The value range for the abovementioned six quantities for 100-mm thick insulator was extremely large: 10–27 dB, 33–52 dB, 0.20–0.78, 3.0–2700 kPa s/m^2, 1.5–730 MN/m^3, and 15–36 dB, respectively. Closed-pore materials usually carried worse acoustic properties than open-pore materials. Unexpectedly, lower thermal conductivity was associated with worse acoustic performance of two acoustic quantities. The study is the broadest acoustic investigation of thermal insulators because of the large number of studied acoustic quantities and insulator types. The study provides strong evidence that the choice of thermal insulator material plays an important role in the acoustic properties of the structural application. Manufacturers should consider declaring all six acoustic quantities to facilitate design.

1. Introduction

1.1. Thermal insulation

Providing adequate thermal insulation on building envelopes is the most important means to minimize energy consumption considering the building's lifecycle. Therefore, thermal insulation requirements for building envelopes have increased strongly during the last decades. For example, in the Nordic countries, the mean thickness of thermal insulation in residential buildings has doubled in 50 years. For example, common mineral wool thickness in Finnish façade walls was 125 mm in 1970, while in 2022, it is 250 mm.

Thermal insulators in façade envelopes (wall, roof, door, base floor) were first used in cold countries to keep the heating energy indoors. Also, the ducts of forced ventilation require wrappings to avoid thermal loss and to reduce noise radiation. Nowadays, thermal

* Corresponding author. Tel. +358 40 5851 888
E-mail address: valtteri.hongisto@turkuamk.fi (V. Hongisto).

https://doi.org/10.1016/j.jobe.2022.104588
Received 25 January 2022; Received in revised form 25 April 2022; Accepted 26 April 2022
Available online 10 May 2022

insulators are increasingly used also in warm countries to save energy used for air conditioning [1]. Furthermore, cold liquid pipes (air conditioning liquids, water) require thermal wrappings to avoid condensation and to reduce noise radiation. Therefore, thermal insulators are of high interest in many countries and applications.

Ref. [2] presented a state-of-the-art of thermal insulators used in Europe. At that time, the thickness of thermal insulation used in façade walls varied from 50 mm (South Europe) to 225 mm (North Europe). The materials could be divided into inorganic (foam glass, glass wool, stone wool), organic (expanded EPS and extruded XPS polystyrene, polyurethane foam, cork, melamine foam, phenol foam, sheep wool, cotton wool, coconut, fibers, cellulose), combined (siliconated calcium, gypsum foam, wood-wool), and new technology materials (transparent and dynamic materials). Furthermore, Ref. [1] reviewed the literature concerning the most typical thermal insulator materials used in Asia. Insulators were available as blankets (batts or rolls), loose-fill blown-in or poured-in layers, rigid boards, sprayed-in-place layers, or foamed in-place layers. The insulators' raw materials were usually stone wool (stone fibers), fiberglass (recycled glass fibers), polyethylene, cellulose (recycled paper), perlite (natural glassy volcanic stone), vermiculite (natural mineral), and expanded or extruded polystyrene. Ref. [3] extended this list by, e.g., hemp, kenaf, flax, and recyclable textile. It is well known that plant straw and sawdust were used to solve thermal insulation problems before industrial insulators were available. Because sustainable building materials are increasingly developed, it is expected that the number of alternative thermal insulation materials increases in the future.

The thermal insulation requirement for a façade wall can also be reached with monolithic load-bearing materials such as thick massive timber. However, multilayered constructions are mostly used since they can be optimized with respect to, e.g., cost, weight, thickness, thermal insulation, sound insulation, visual appearance, and fire protection. In such constructions, industrial light thermal insulator layers are used, and they are encapsulated by boards or slabs.

1.2. Sound insulation

Requirements concerning environmental noise protection have increased since the 1990's, because there is very strong evidence that excessive indoor noise level causes adverse health effects due to noise annoyance and worsened quality of sleep [4]. For example, in Finland, the A-weighted equivalent sound pressure level (SPL), $L_{Aeq,T}$, indoors shall not exceed 35 dB during daytime hours (07–22, T = 15 h) and 30 dB during nighttime hours (22–07, T = 9 h) [5]. Properly designed façade constructions (consisting of a window, balcony door, and a solid wall) can reduce the SPL of environmental noise transmitting indoors even by 45 dB L_{Aeq}. Therefore, residential buildings can be built in areas, where SPL of the environmental noise is at most 75 dB L_{Aeq}. In the most demanding cases, the façade components, i.e., windows, doors, walls, roofs, balcony glazings, and ventilation routes, must be optimized regarding their airborne sound insulation.

Because the thermal insulator is usually located between boards or slabs, the façade wall behaves as an acoustic double construction. It has been shown that a highly sound-absorbing material entirely filling the cavity significantly reduces the reverberation inside the cavity compared to the situation where the cavity is partially filled, empty, or filled with material with reduced sound-absorption properties [6]. Therefore, the selection of the thermal insulator material significantly affects the façade wall sound insulation. From the perspective of building economy, it is beneficial to choose a thermal insulator type with superior acoustic properties to reach a specific sound insulation requirement.

The acoustic performance of a building is described by several primary quantities. The primary acoustic quantities used in building regulations or other target values are (I−III):

I. Airborne sound insulation between rooms or between outdoors and indoors (façade). This is primarily based on the sound reduction index of the separating elements (e.g., walls, floors, doors, windows, small elements, floors, and ventilation outlets) and their junctions;
II. Impact sound insulation between spaces. This is primarily based on the normalized impact sound pressure level of intermediate floors and stairs;
III. Reverberation time of rooms requiring high speech intelligibility or noise control (e.g., auditoria, meeting rooms, stairways, engine rooms, and open-plan offices).

On the other hand, these primary quantities can be designed by using several secondary or tertiary quantities of the materials. Resilient materials (open-pore or closed pore materials) are frequently used as a part of the construction to reach the requirements of building regulations. Resilient materials carry properties that are called secondary quantities (IV–V):

IV. Sound absorption coefficient, which is used to predict quantity III, and to predict the values of quantities I−II in the case of multilayered constructions involving resilient layers;
V. Reduction of impact sound pressure level of floor coverings or floor toppings, which is used to predict the values of quantity II.

Moreover, at least the following tertiary quantities (VI−X) are needed to predict the values of quantities I–V:

VI. Surface mass of a rigid layer is used to predict the values of quantities I, II, and V;
VII. Young's modulus of rigid slabs (boards) is used to predict the values of quantities I, II, and V;
VIII. Acoustic total loss factor of rigid slabs (boards) is used to predict the values of quantities I, II, and V;
IX. Airflow resistivity of a resilient layer is used to predict the values of quantities I–V; and
X. Dynamic stiffness per unit area of a resilient layer is used to predict the values of quantities I, II, V, if the layer is adhesively connected to surface boards (e.g., floating floors, and sandwich constructions).

Previous studies reporting acoustic properties of thermal insulators have usually focused on single acoustic quantities. Ref. [3] reported the airflow resistivity [Pa·s·m^{-2}] for many insulator materials listed above. However, they did not report any values of the primary acoustic quantities. Ref. [7] reported the dynamic stiffness per unit area of eight insulator types. Sound absorption coefficients of thermal insulators have been experimentally studied in, e.g., Refs. [8,9]. The microstructure of different thermal insulator materials varies a lot, which affects the values of quantities VI–X. For example, higher airflow resistivity was negatively associated with sound absorption performance [10]. Higher sound absorption performance is known to be positively associated with sound reduction index if the material is placed in the cavity between two building boards or slabs [6]. In sandwich constructions, the thermal insulator is adhesively installed between two boards or slabs. For example, the sound reduction index of sandwich façade constructions suffers from poor sound insulation at the dilatation resonance frequency, which often appears within 100–3150 Hz [11]. The dilatation resonance occurs also with floating floors [12]. Increased dynamic stiffness per unit area is associated with reduced impact sound insulation of floating floors [12,13].

As explained above, acoustic requirements and quantities in buildings are very multifaceted. To our knowledge, there are no previous studies which have investigated different thermal insulator materials with respect to several acoustic quantities. It is important to improve the broad understanding of acoustic properties of thermal insulators to facilitate construction science and design.

When the building locates in a noisy area, both the thermal insulation and sound insulation of the façade need to be simultaneously considered. Therefore, it is important to know the association between thermal insulation and acoustic performances. Combining these two important properties of building physics into the same research is a novel approach and benefits the economic design of a building. Precise knowledge of thermal insulators' acoustic behavior is also important to be able to develop sustainable constructions. The design of the acoustic properties of a façade of a specific building is often based on mathematical prediction models. There are relatively simple and functionable analytic models to predict the sound reduction index as a function of frequency [14]. However, the model cannot be applied without knowing the basic material properties of slabs/panels (quantities VI, VII, and VIII), thermal insulator layer (IV, IX, and X) or stud properties (stud division, stud type, dynamic stiffness) included to the wall. It is important that also thermal insulator manufacturers declare the fundamental acoustic material properties in product specifications. However, such a progress requires scientific evidence that these acoustic properties need to be available.

1.3. Purpose

Our first purpose is to experimentally determine the acoustic properties for 13 thermal insulator types (or materials) with three thicknesses to outline the range of acoustic performances. All studied insulator products were commercially available in 2021. The studied acoustic quantities are.

- sound reduction index of bare insulator,
- sound reduction index of encapsulated insulator (inside a double construction), and
- normal incidence sound absorption coefficient,
- airflow resistivity,
- dynamic stiffness per unit area,
- reduction of impact sound pressure level in a floating floor.

Our second purpose is to analyze, how these six acoustic quantities, material density, and thermal conductivity, are associated with each other.

2. Materials and methods

2.1. Thermal insulators

Our research includes 13 different **insulator types**. They were chosen according to the following criteria:

Table 1
The studied insulator types and their thermal conductivity, λ, density, ρ (involves the air pores), and density of the solid raw material, ρ'.

	Insulator type (material)	λ [W/mK]	ρ [kg/m^3]	ρ' [kg/m^3]
1	Ultra-low density stone wool slab	0.044	25	2500
2	Low density stone wool slab	0.036	25	2500
3	Medium density stone wool slab	0.033	75	2500
4	High density stone wool slab	0.037	100	2500
5	Ultra-low density glass wool roll	0.040	11	2500
6	Low density glass wool slab	0.035	16	2500
7	Medium density glass wool slab	0.033	70	2500
8	Cellulose slab	0.039	37	1500
9	Wood fiber slab	0.038	50	600
10	Expanded polystyrene board	0.036	18	1050
11	Polyisocyanurate board	0.022	30	40
12	Phenolic foam board	0.020	30	1070
13	Cellular glass board	0.036	100	200

- Each insulator type is commercially available and frequently used in Europe;
- Insulator types based on same raw material must have essentially different density;
- The insulator type is specifically used because of its thermal insulation property – massive impervious constructions carrying thermal insulation, such as timber or masonry, were not included.

The following materials are frequently used as thermal insulators in Europe: stone wool, glass wool, cellulose, wood fiber, polystyrene, polyisocyanurate, phenolic, and cellular glass. Therefore, all of them were included in our experimental study.

Each insulator type is based on a different raw material carrying a specific bulk density, and bulk thermal conductivity. Because thermal insulation requirements of building envelopes vary according to regional regulations for different building uses, most insulator types are available at different thicknesses. Thereby, we come to the term **insulator products**. It represents an insulator type carrying a specific thickness. We tested three thicknesses for each insulator type to improve the reliability of our conclusions and to understand the effect of thickness on the acoustic performances. Thereby, our study covers 39 insulator products.

The studied insulator types are described in Table 1. They are all commercially available and very popular. Most of the acoustic properties were determined for three thicknesses, d [m]: 50, 100, and 200 mm. All insulator types were available at our main thickness of interest, i.e., $d = 100$ mm. Only two insulator products were available at 200 mm. The rest of the 200-mm thick insulator products consisted of two layers of a 100-mm thick product.

Some of the insulator types were not available at the desirable thicknesses, 50 mm or 200 mm. One 50 mm insulator product had to be sliced from a 100-mm thick insulator product. One insulator type was not available at 50 mm nor could be sliced from a 100-mm thick insulator product without losing inherent surface properties of that insulator type. Two insulator types were not available at $d =$ 200 mm. Therefore, an insulator product nearest to the desired thickness had to be chosen in these cases. It was better to accept these minor deviations (insulator products 11_70, 11_150, and 12_140) since our study is explorative: exclusion of two insulator types from the survey would have reduced the coverage of our study.

Thermal insulation performance of the insulator type (irrespective of its thickness) is described by thermal conductivity λ [W/m·K]. It describes the thermal power transmitted through a 1-m-thick material layer, when the temperature difference between the two surfaces is 1 K and the area is 1 m^2. Thermal conductivity is used as an inherent property of the insulator type. Low value denotes high thermal insulation performance. Thermal resistance R_{th} [m^2·K/W] describes how well an insulator product resists thermal flow. It is

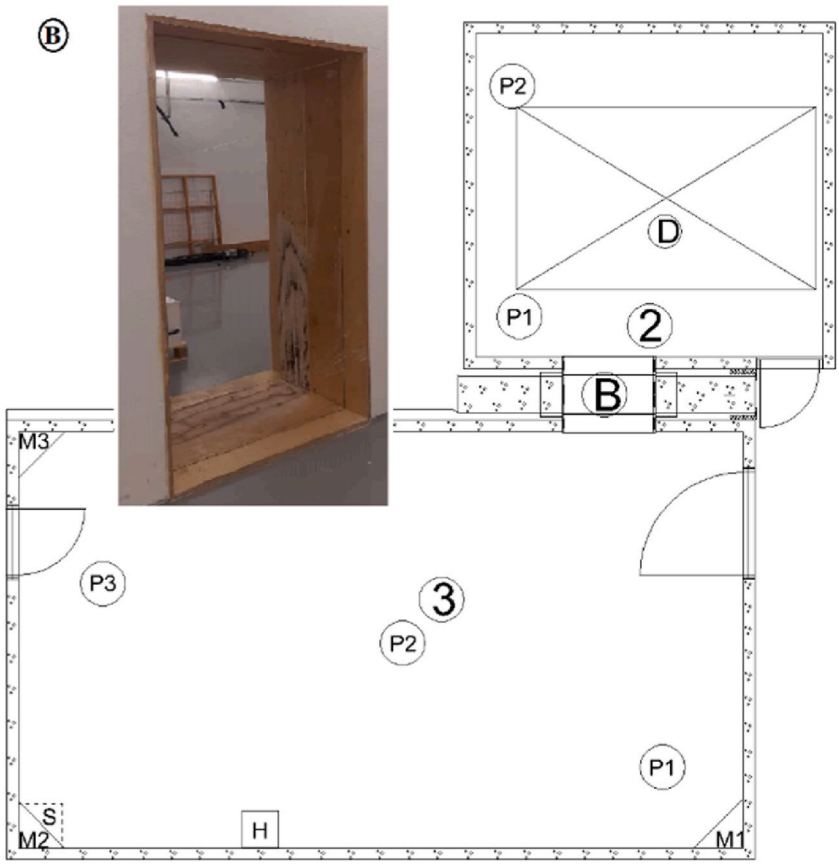

Fig. 1. The layout of the laboratory for sound reduction index measurements. The laboratory involves the source room (3), the receiving room (2) and the test opening (B) between them. Five loudspeakers (M1−M3, S, H) were used to produce the test signal. The photograph shows the test opening without a sample.

calculated by

$$R_{th} = \frac{d}{\lambda} \tag{1}$$

where d [m] is the thickness of the product. The thermal properties were obtained from product specifications.

2.2. Sound reduction index for bare insulator

Bare thermal insulator layers are never used alone in façades since they usually carry weak properties regarding, e.g., mechanical strength, moisture protection, air permeability and sound insulation. Therefore, thermal insulators are usually installed between boards or slabs.

Instead of façades, bare thermal insulators are frequently used in construction linings and duct wrappings. In such applications, the airborne sound insulation (physical quantity is sound reduction index, SRI) of bare thermal insulation is relevant. The lining or wrapping reduces the noise emission simply by the SRI value of the bare insulator product [15]. Measurement of the SRI of bare insulator products was therefore justified.

The SRI of 39 insulator products was determined according to ISO 10140–2 [16]. Single-number quantities were determined according to ISO 717–1 [17]. The test laboratory is described in Fig. 1. The volumes of the source and the receiving room were 201 and 64 m^3, respectively. Loud pink noise was produced in the source room using five independent signal generators (Behringer Ultra curve DEQ 2496), three stereo amplifiers (QSC RMX 850, 850, 2450), and five loudspeakers. The sound pressure levels (SPL) were measured simultaneously in the source room, L_1 [dB], and in the receiving room, L_2 [dB], using condenser microphones (Brüel & Kjaer 4165, Denmark), when the loudspeakers were on. The microphones were installed on rotating microphone booms (Brüel & Kjaer 3923, Denmark). The radius of rotation was 1.00 m and the time of one complete rotation was 64 s. The SPL of background noise in the receiving room, $L_{2,B}$ [dB], was measured immediately after the measurement of L_2.

The reverberation time (T_2) was determined in the receiving room according to the engineering method of ISO 3382–2 [18]. Pink noise was produced to receiving room with the analyzer and amplified with amplifier (QSC 900 W USA). Two fixed loudspeaker positions were used, and the microphone was placed in three positions. Reverberation time was determined using two averaged decay signals from the decay range of −5 to −25 dB in each measurement. The reverberation time of an empty receiving room was approximately 1.4, 2.1, 2.4, 3.2, 3.4, 2.6, and 1.6 s for octave bands 63, 125, 250, 500, 1000, 2000, and 4000 Hz, respectively. The reverberation time was measured for every sample since the sample slightly affected the reverberation time.

The measurement equipment was checked before and after the measurements using a sound level calibrator (Brüel & Kjaer 4231, Denmark). All analyses were made using the same real-time analyzer (Norsonic Nor 121, Norway).

The SRI was determined by [16]

$$R = L_1 - L_{2,c} + 10 \cdot \log_{10}\left(\frac{S}{A_2}\right) \tag{2}$$

where S [m^2] is the area of the tested product and $L_{2,c}$ [dB] is the SPL in the receiving room involving the background noise correction. Background noise correction was not needed in any of our measurements. The equivalent absorption area in the receiving room, A_2 [m^2], was determined by [16]

$$A_2 = \frac{0.16 \cdot V_2}{T_2} \tag{3}$$

where V [m^3] is the volume of the receiving room.

Each test sample was installed in a test opening of area 2.55 m^2 (height 2100 mm and width 1215 mm). Samples were prepared from several pieces since the manufactured board size was usually much smaller than the test opening. The material was installed between steel corner battens spaced by the thickness of the current material (Fig. 2a).

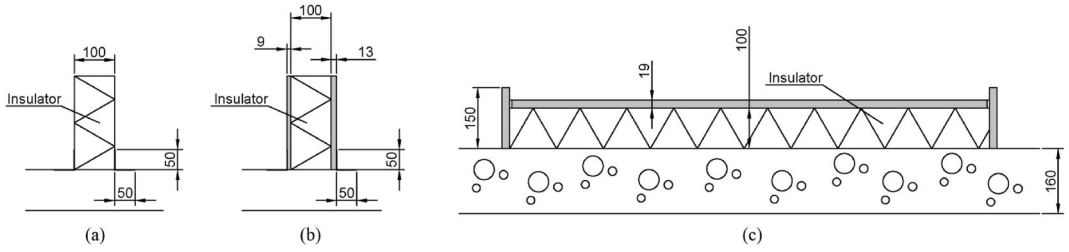

Fig. 2. Installation of test sample during sound insulation tests. (a) Bare insulator during airborne sound insulation test R_1. Three thicknesses were tested for each thermal insulation material, making altogether 39 tests. (b) Encapsulated insulator during airborne sound insulation test R_2. The boards were 9 mm birch veneer (6.0 kg/m^2) and 13 mm gypsum board (9.9 kg/m^2). c) Insulator placed under a building board during impact sound insulation test (ΔL). The board was 19 mm birch veneer (16.4 kg/m^2).

2.3. Sound reduction index for enveloped insulator

The SRI of every insulator type was also determined in a setup where the insulator product was enveloped by two building boards (9 mm veneer 6.0 kg/m^2, and 13 mm gypsum board 9.9 kg/m^2). The measurements were conducted in the same way as in Sec. 2.2 using the same sample area and test opening. Both boards were sealed on the edges to avoid sound leakages. This test was only conducted for insulator products with 100 mm thickness. The installation is shown in Fig. 2b. The installation was loose: the board was not glued to the insulator product nor compressed to avoid the situation where the insulator acts as a mechanical spring between the boards.

2.4. Sound absorption coefficient

The normal incidence sound absorption coefficient, α_0, was determined using the transfer function method and an impedance tube according to standard ISO 10534–2 [19]. The measurement system is shown in Fig. 3. The frequency-dependent normal incidence sound absorption coefficient, α_0, is determined by

$$\alpha_0(k_0) = 1 - \left| \frac{H_{12}(k_0) - e^{-jk_0 s}}{e^{jk_0 s} - H_{12}(k_0)} \cdot e^{2jk_0 x_1} \right|^2 \tag{4}$$

where k_0 (1/m) is the complex wavenumber in air ($k_0 = k_0' - jk_0''$, $k_0' = 2\pi f/c_0$), f [Hz] is the frequency of sound, c_0 [m/s] is the speed of sound in air, s [m] is the distance between microphones 1 and 2, and x_1 [m] is the distance from the sample surface to microphone 1 (see distances in Fig. 3). The exponential terms are frequency-dependent constants since the microphone positions are constantly the same in the impedance tube. The only measurable quantity is the transfer function from microphone 1 to 2, H_{12} [-] defined by

$$H_{12}(k_0) = \frac{p_2(k_0)}{p_1(k_0)} \tag{5}$$

where p_1 [Pa] and p_2 [Pa] are the Fourier transformed pressures at microphone positions 1 and 2 (k_0-dependent). Since the microphones 1 and 2 are not perfectly phase matched but they carry a minor phase difference φ, the transfer function was determined twice (I and II) by interchanging the microphone positions and the phase-corrected transfer function to be applied in Eq. (4) is the geometric average of the two setups:

$$H_{12} = \sqrt{H_{12}^{I} \cdot H_{12}^{II}} \tag{6}$$

The internal diameter of the impedance tube (B&K 4206) and the diameters of the cylindrical test samples were 63.5 mm. The samples were prepared using water cutting. A real-time, two-channel analyzer (Norsonic 840A) was used to determine the H_{12}. The spacing of the 1/4″ microphones (B&K Type 2670) was $s = 31.8$ mm. The exact frequency range of the FFT analysis was 100–3146 Hz. The reported results for the 100 Hz and 3150 Hz 1/3-octave bands are based on only one half of the 1/3-octave band, i.e., on frequency ranges of 100–114 Hz and 2800–3146 Hz, respectively. A MATLAB computer program was used to calculate α_0.

Two samples were prepared from each insulator product and their average value is reported. One single-number quantity was defined: mean sound absorption coefficient, α_M, within 100–3150 Hz.

2.5. Airflow resistivity

The airflow resistivity σ [Pa·s/m^2, N/m^4·s] was measured according to ISO 9053–1 [20]. The measurement system is shown in

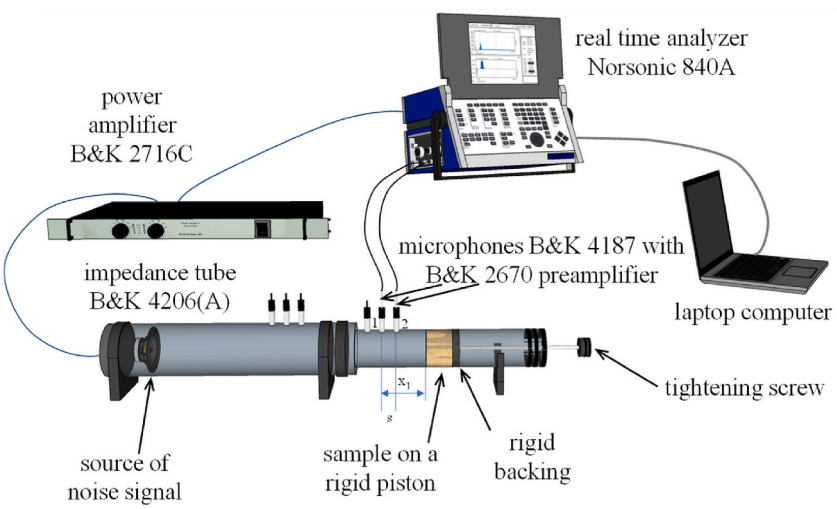

Fig. 3. The setup used for the measurement of normal-incidence sound absorption coefficient.

Fig. 4. Two samples (diameter 63.5 mm) used in the sound absorption tests were used. Petroleum jelly was applied to the sides of the coated wools to improve the fit and to prevent any side leaks. A controlled unidirectional airflow, created using a rotary vacuum pump (Busch Type SV 1003), was passed through the piece of material inside a circular cylinder 63.5 mm in diameter. The pressure drop over the test material, Δp [Pa], was measured using a pressure micromanometer (Swema 3000md). The volumetric airflow rate, q_v [m^3/s], was measured with rotameter involving a flow rate control (Tokyo Keiso NP-G25). Eight airflow rates within 2.5 and 9 L/min were used. In each airflow rate, the airflow resistivity was determined from

$$\sigma = \frac{\Delta p \cdot A}{q_v \cdot d} \tag{7}$$

where A [m^2] is the area of the sample perpendicular to the flow, and d [m] is the sample thickness. The reported specific airflow resistance was determined by extrapolating to an airflow rate of 0.095 L/min, which corresponds to airflow speed 0.5 mm/s. For a specific homogeneous material, the value of σ is independent of thickness.

An exception to the abovementioned procedure was made with insulator products having very high airflow resistivity (closed-pore insulators). Some of them were extremely airtight and we believe that most of the air was flowing via the seams between the sample and the sample tube. They were measured using a single airflow rate but using multiple installations and high attention was paid to the sealing of the sample. We believe that the uncertainty of high airflow resistivity values is much higher for closed-pore insulator products than for the open-pore insulator products.

Airflow resistivity is used in several prediction models to predict the sound absorption coefficient [10]. If the value is multiplied by the thickness of the insulator product, the outcome is specific airflow resistance Ξ [Pa·s/m]. This quantity depends on material thickness unlike σ. For clarity, we reported both σ and Ξ. Since we conducted the measurements for all 39 products using different material pieces, the reported values of σ are not constant over different thicknesses although they are made of the same material, and σ should theoretically be independent of thickness. The reason is that the quality of the material slightly varies between the material pieces. In addition, we expect that values exceeding 1000 kPa·s/m^2 can be unreliable: the measured airflow can be contaminated by leaks around the sample and the values do not necessarily represent inherent material property.

2.6. Dynamic stiffness per unit area

Dynamic stiffness per unit area s' [Pa/m, N/m^3] was determined according to ISO 9052–1 [21]. It describes the resiliency of the insulator product perpendicular to the horizontal surface. The measurement system is shown in Fig. 5.

Three samples of 200 × 200 mm were cut from each product. Each sample was separately tested, and the mean is reported. The sample was placed against rigid, heavy floor (surface mass >600 kg/m^2). A load plate (steel plate 200 × 200 mm, total mass $m_L = 7.8$ kg) was installed on top of the sample so that the floor (having "infinite mass"), the sample, and the load formed a mass-spring-mass system. The load plate was excited vertically by an electromagnetic shaker (Brüel&Kjær 4813) using a rod. A force transducer was installed between the rod and load plate (Brüel&Kjær 8200). The test signal was white noise produced by signal generator (Norsonic 840A). The signal was amplified (Brüel&Kjær 2707) before feeding to the shaker. Vibration of the load plate was measured by accelerometer (Brüel&Kjær 4370). The accelerometer signal was fed back to the acoustic analyzer (Norsonic 840A). At the resonance frequency f_r, the load plate begun to vibrate strongly (see Fig. S1 in Supplementary data showing a typical acceleration spectrum). The resonance frequency was determined from the peak position in the FFT spectrum. The FFT resolution was 0.244, 0.488, or 0.977 Hz depending on the resonance frequency. The apparent dynamic stiffness per unit area, s'_t [N/m^3], of the test sample at the resonance frequency was determined by

$$s'_t = 4\pi^2 m_L f_r^2 / A \tag{8}$$

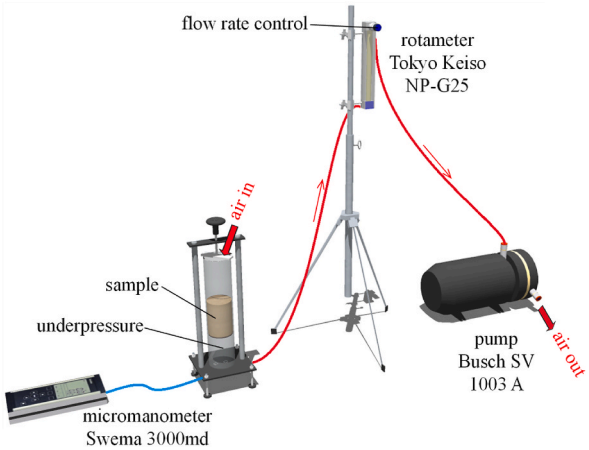

Fig. 4. Description of the airflow resistivity measurement setup.

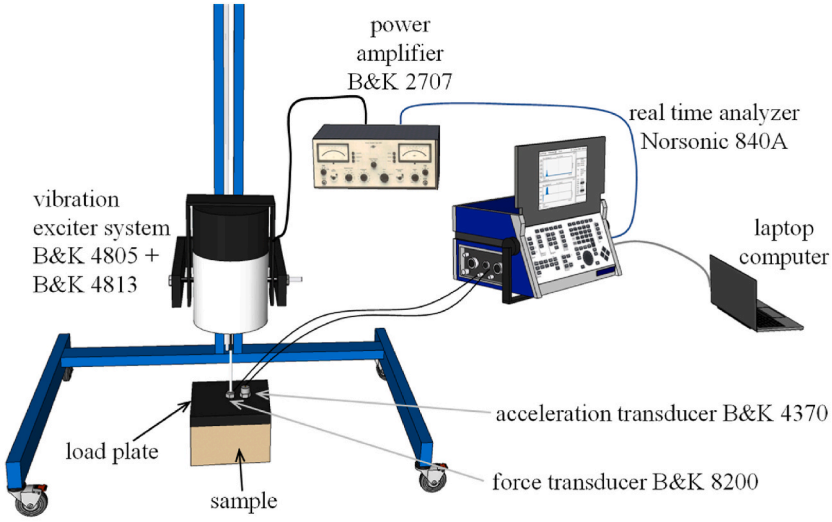

Fig. 5. The setup used for the measurement of dynamic stiffness per unit area.

where A [m^2] is the area of the sample against the load plate (0.04 m^2).

Vibrating air inside the sample pores easily escapes to the surrounding space in the measurement setting described above since the insulator area is small and vertical borders of the sample are not isolated from the surrounding space. In floor setting, the insulator is located under a floating floor slab being typically 10 m^2 or larger and the air cannot escape to the surrounding space. The compressed air trapped inside the insulator forms a secondary stiffness component, called the dynamic stiffness of air, s'_a [N/m^3]. It is calculated by

$$s'_a = \frac{p_0}{d(1-\rho/\rho')} \tag{9}$$

where p_0 [Pa] is the atmospheric pressure (101300 Pa), d [m] is the thickness of the sample under the applied static load, ρ [kg/m^3] is the density of the insulator product, and ρ' [kg/m^3] is the density of the solid raw material of the insulator. Both densities are given in Table 1. Finally, the dynamic stiffness of the material under floating floor (where air is trapped within the insulator), s', is obtained by

$$s' = s'_t + s'_a \tag{10}$$

ISO 9052–1 [21] proposes that s'_a is ignored outside the flow resistivity range 10–100 kPa·s/m^2. Because the scientific reasoning of this procedure is vague, and we determined the airflow resistivity only in perpendicular direction, not in lateral direction, we reported the s' values using Eq. (10) but we also reported the values of s'_a and s'_t.

Higher resiliency (lower s') is associated with lower resonance frequency in floating floors (impact sound insulation, airborne sound insulation) and sandwich constructions (airborne sound insulation). Dynamic stiffness, s' [N/m^3], is used to describe the properties of resilient materials used in floating floors. The mass-spring-mass resonance frequency, f_0 [Hz], of a floating floor is calculated by

$$f_0 = \frac{1}{2\pi}\sqrt{\frac{s'}{m'}} \tag{11}$$

where m' [kg/m^2] is the mass per unit area of the floating slab. For example, the impact sound insulation performance of a floating floor, i.e., the weighted reduction of impact sound pressure level, ΔL_w [dB], can be coarsely predicted by Ref. [13]; when s' and m' are known.

Quantity s' is essential also for the SRI of constructions (walls, doors, floating floors) having a sandwich structure, where the thermal insulator is mechanically tied to the surrounding boards or slabs (compressed and/or glued). In such a system, the resilient material acts as a mechanical spring and the wall forms a mass-spring-mass system. When the material is loosely placed inside the cavity between boards or slabs, the material is not acting as a spring. The dilatation resonance frequency of sandwich constructions, f_d, is calculated by Ref. [11]:

$$f_d = \frac{1}{\pi}\sqrt{s'\frac{(m'_1+m'_2)}{m'_1 m'_2}} \tag{12}$$

where m'_1 and m'_2 [kg/m^2] are the surface masses of the boards 1 and 2, respectively.

Nine insulator products of our study were very soft, which makes them inadequate for floating floors but adequate in vertical constructions. ISO 9052–1 is not designed for measuring extremely resilient insulator products since the load plate compresses the

insulator product so much that the actual thickness during the test deviates from the nominal thickness by more than 10%. Therefore, we assume that measurement results under 1 MN/m^3 have higher uncertainty.

2.7. Impact sound insulation using floating floor setup

Hard insulator types are frequently used, with minor property changes, as the resilient material of floating floors. Therefore, the impact sound insulation performance was also determined in a constant floating floor setup. The floating floor was installed against a heavy-weight reference slab used for testing the performance of flooring materials (160 mm steel-reinforced concrete, 400 kg/m^2). We built a 150-mm-high wooden frame having the same size as airborne sound insulation test: (2110 × 1210 mm) and placed it on the reference slab. The tested insulator product was placed inside the frame and covered by 19 mm birch veneer board (16.4 kg/m^2). The veneer did not touch the frame (3 mm gap). The gap was sealed with duct tape to avoid air leakage.

The reduction of impact sound pressure level, ΔL [dB], of the floating floor was determined according to ISO 10140–3 [22] and ISO 717–2 [23] by

$$\Delta L = L_{2,0} - L_{2,1} \tag{13}$$

where $L_{2,0}$ [dB] is the SPL in the receiving room when the reference slab is bare (no floating floor), and $L_{2,1}$ [dB] is SPL in the receiving room, when the reference slab is covered by the floating floor.

The standard tapping machine (Norsonic 277) was used to produce standard impact sound against the sample. The sound pressure level in the receiving room (volume 64.4 m^3) was measured as in Sec. 2.2. The measurements were repeated two times using two positions of the tapping machine on veneer. Fig. 6 shows the test laboratory and Fig. 2c shows the sample on the reference slab. Reverberation time was determined as in Sec. 2.2.

The test was only made for insulator products having 100 mm thickness. One sample per insulator product was tested.

2.8. Measurement process

The insulator products were delivered in ordinary commercial packages. The amount of each product was determined by the sample amount required in the airborne sound insulation test. The packages were delivered to the laboratory from wholesale in January 2021. The packages were first numbered using the insulator product number (1–39). Then, the product declaration labels of each package were stored, and the package was opened for testing purposes. The basic quantities were recorded (d, m', λ) from the manufacturer's public data sheets. The acoustic quantities were measured in the following principal order: R_1, R_2, DL, s', α_0, and σ. The measurements took altogether three months.

3. Results

The measured single-number values are shown in Table 2 for the 13 insulator types. The range of values for 100 mm thickness is summarized in **Appendix**. The frequency-dependent values are shown in Figs. 7–10. Correlation coefficients between the single-number quantities for the 13 different materials are shown in Table 3. Notation ** indicates a statistically significant linear association between the quantities. Fig. 11 raises some relevant associations from Table 3. The dependence of mean absorption coefficient and weighted SRI on the thickness of insulator type is shown in Fig. 12.

4. Discussion

4.1. Associations between different quantities

This section explores the findings of Table 3 showing linear associations for the 13 insulator types.

Density (or surface mass) was positively associated with the weighted SRI of bare insulator product, R_{W1}, but not with other

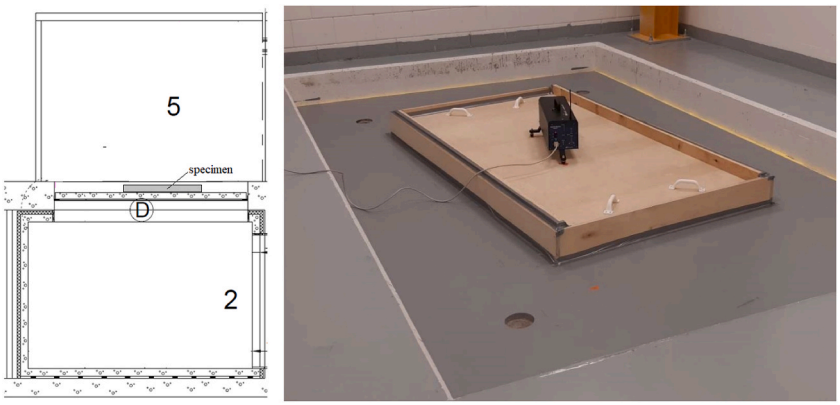

Fig. 6. Description of the measurement of impact sound insulation. Left) Section of the laboratory including the source room (5), the receiving room (2), and the reference slab of area 4100 × 2500 mm (D). Right) A photograph showing the reference slab, sample, and the tapping machine.

Table 2
The measured single-number values of the 39 tested products (ID). The product name of each insulator type 1–13 is given in Table 1. Thickness, d, surface mass, m', thermal resistance, R_{th}, mean absorption coefficient, α_M, dynamic stiffness per unit area, s', reduction of weighted impact SPL, ΔL_w, weighted sound reduction index of bare insulator product, R_{w1}, weighted sound reduction index of encapsulated insulator product, R_{w2}, and airflow resistivity, σ. Table S1 (see Supplementary data) reports the values of s'_t, s'_a, and Σ.

ID	d [mm]	m' [kg/m^2]	R_{th} [m^{2}K/W]	α_M	s' [MN/m^3]	ΔL_w [dB]	R_{w1} [dB]	R_{w2} [dB]	σ [kPa·s/m^2]
1_50	50	1.3	1.14	0.52	9.2		7		8.1
2_50	50	1.3	1.39	0.56	4.2		8		13
3_50	50	3.8	1.52	0.60	6.1		13		33
4_50	50	5.0	1.35	0.59	16		15		50
5_50	50	0.6	1.19	0.44	7.8		6		3.8
6_50	50	0.8	1.43	0.52	4.5		8		12
7_50	50	3.5	1.52	0.58	3.0		9		17
8_50	50	1.9	1.28	0.55	3.7		7		9.4
9_50	50	2.5	1.32	0.50	6.6		5		8.8
10_50	50	0.9	1.39	0.16	71		12		4200
11_70	70	2.1	3.18	0.16	17		15		3900
12_50	50	1.5	2.50	0.16	23		19		5500
13_50	50	5.0	1.39	0.19	940		22		2000
1_100	100	2.5	2.27	0.73	2.8	36	11	51	6.6
2_100	100	2.5	2.78	0.75	2.6	36	15	51	12
3_100	100	7.5	3.03	0.70	2.8	35	21	50	31
4_100	100	10.0	2.70	0.68	12	32	22	50	33
5_100	100	1.1	2.38	0.72	4.2	33	11	50	3.0
6_100	100	1.6	2.86	0.78	2.2	36	15	52	10
7_100	100	7.0	3.03	0.73	1.5	36	17	51	16
8_100	100	3.7	2.56	0.73	1.8	35	12	50	11
9_100	100	5.0	2.63	0.71	3.0	34	10	50	5.9
10_100	100	1.8	2.78	0.27	45	20	16	38	530
11_100	100	3.0	4.55	0.22	14	16	15	33	2600
12_100	100	3.0	5.00	0.20	36	15	20	34	2700
13_100	100	10.0	2.78	0.26	730	15	27	35	68
1_200	200	5.0	4.55	0.87	1.5		19		6.2
2_200	200	5.0	5.56	0.82	1.2		25		11
3_200	200	15.0	6.06	0.69	1.3		31		28
4_200	200	20.0	5.41	0.58	8.5		28		49
5_200	200	2.2	4.76	0.85	1.7		18		2.5
6_200	200	3.2	5.71	0.86	1.1		23		6.5
7_200	200	14.0	6.06	0.78	0.72		26		17
8_200	200	7.4	5.13	0.83	0.92		19		11
9_200	200	10.0	5.26	0.85	1.5		17		6.0
10_200	200	3.5	5.56	0.30	24		21		510
11_150	150	4.5	6.82	0.21	13		15		1300
12_140	14	4.2	0.70	0.20	31		22		1400
13_200	200	20.0	5.56	0.33	430		31		190

quantities. This agrees with the model of Ref. [15]; according to which the SRI of blankets depends mainly on surface mass and airflow resistivity, when the material thickness is smaller than one-tenth of wavelength in the material.

Thermal conductivity, λ, was negatively associated with airflow resistivity, σ. This finding suggests that the lower is the thermal insulation, the higher is the airflow resistivity. This may be explained by the fact that insulator types 1–9 have lower airflow resistivity than insulator types 10–13. Two insulator products (11_100 and 12_100) had extremely high airflow resistivity. They are prone to higher uncertainty since the values may be caused just by air leaks passing the sample. If these two insulator products are ignored from the analysis, the association between λ and σ disappears.

Mean absorption coefficient, α_M, was negatively associated with airflow resistivity, σ. That is, lower σ predicts higher α_M. This agrees with Ref. [10], who experimentally validated different sound absorption prediction methods assuming this association.

Mean absorption coefficient, α_M, was positively associated with reduction of weighted impact SPL, ΔL_w. However, this is probably not a primary association. Open-pore insulator types (1–9) are systematically more resilient (lower s') than the closed-pore insulator types (10–13). Therefore, we assume that the larger resiliency associated with open-pore insulators might be the actual reason for the association.

Mean absorption coefficient α_M was positively associated with the weighted SRI of encapsulated insulator product, R_{w2}. Poor absorption in the cavity leads to stronger reverberation which reflects as the reduction of SRI. The finding agrees with the literature giving simple models how the absorption coefficient explains the SRI [14,24]. However, our study provides novel data since it contains both several open-pore (1–9) and several closed-pore insulator types (10–13). Our results suggest that closed-pore insulator types have smaller R_{w2} than open-pore insulator types. Although the closed-pore insulator types have smaller thermal conductivity than the open-pore insulator types, the loss in R_{w2} performance must be compensated by other means, such as using more mass in the surrounding building boards.

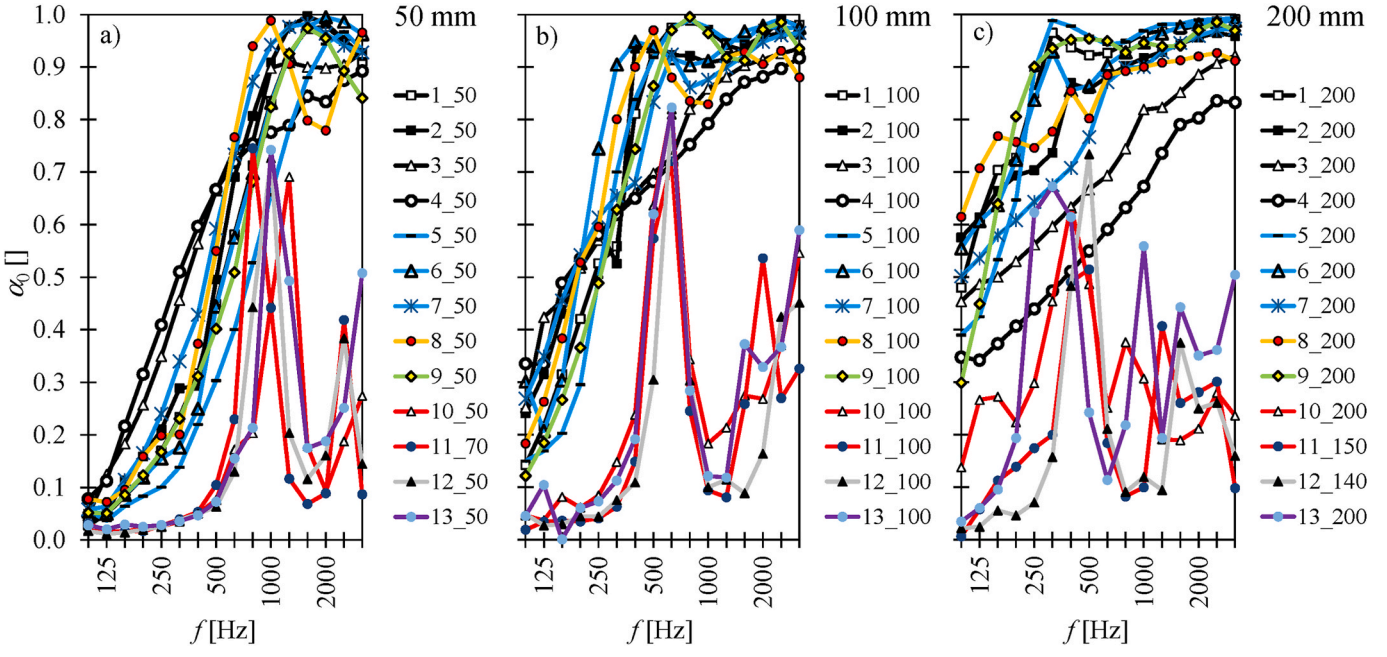

Fig. 7. Absorption coefficient, α_0, as a function of frequency, f, for the three nominal material thicknesses tested for each insulator type: a) 50 mm, b) 100 mm and c) 200 mm. The product name of each insulator type is given in Table 1. Actual thickness disagrees with nominal thickness for products 11_70, 11_150 and 12_140. Numerical values are shown in Table S2 (Supplementary data).

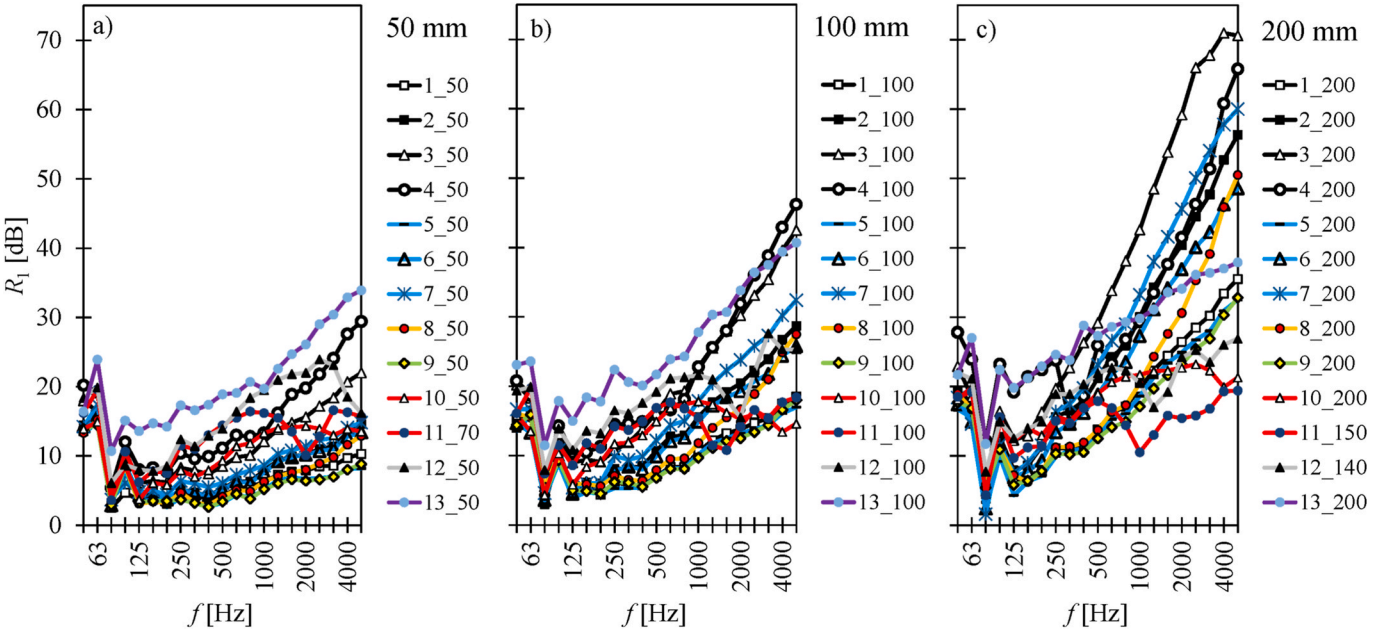

Fig. 8. Sound reduction index (airborne sound insulation) of bare insulator product, R_1, as a function of frequency, f, for the three nominal thicknesses: a) 50 mm, b) 100 mm, and c) 200 mm. The product name of each insulator type is given in Table 1. Actual thickness disagrees with nominal thickness for products 11_70, 11_150 and 12_140. Numerical values are shown in Table S3 (Supplementary data).

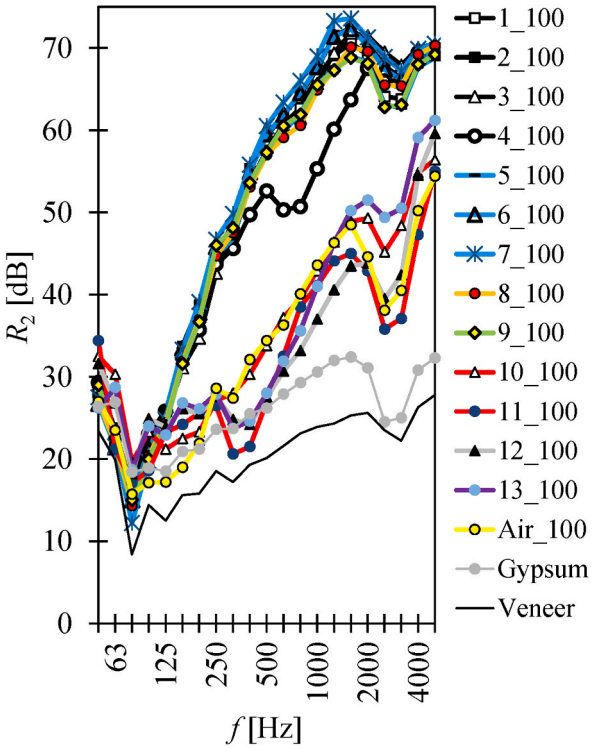

Fig. 9. Sound reduction index (airborne sound insulation) of encapsulated insulator product, R_2, as a function of frequency, f, for the insulator types with thickness 100 mm. The product name of each insulator type 1–13 is given in Table 1. Comparison is made to the situation when the 100-mm cavity between gypsum and veneer is filled with air (Air_100) to indicate the benefit of adding the insulator to the cavity. The sound reduction indices of bare gypsum and bare veneer are also shown. Numerical values are shown in Table S4 (Supplementary data).

Dynamic stiffness per unit area, s', was not statistically and negatively associated with ΔL_w within the whole sample of 13 insulator types. This finding seems to contradict with general understanding of the impact sound insulation of floating floors [12,13]. The reason for the unexpected finding was that insulator type 13 was exceptionally rigid. The reported s' value may also contain uncertainties since the test method is not designed for hard materials. If this insulator product is ignored in the analysis, the correlation coefficient became statistically highly significant (−0.80), which agrees with expectations.

Dynamic stiffness per unit area, s', showed a weak association with R_{w1}. This finding is, however, a coincidence: there is no reason to expect that these quantities should be linked since the insulator was not mechanically compressed while R_{w1} was tested.

Airflow resistivity, σ, was negatively associated with ΔL_w. The finding may be caused by the fact that open-pore materials with small σ happen to be more resilient (low s') than closed-pore materials having high σ (high s'), while s' is negatively associated with ΔL_w.

Airflow resistivity, σ, was negatively associated with R_{w2}. This reflects the same as the abovementioned association between α_M and R_{w2} since α_M is strongly associated with σ.

4.2. Absorption coefficient

The normal incidence sound absorption coefficient, α_0, was determined using three thicknesses of each insulator type. The effect of thickness on α_0 is evident (Fig. 7). Open-pore insulator products have low airflow resistivity σ and they systematically have much higher α_0 than the closed-pore insulator products having higher σ.

In addition to that, the frequency dependency of open-pore insulator products' α_0 clearly deviates from those of closed-pore insulator products. Open-pore insulator products show almost monotonic increase of α_0 as a function of frequency at all three thicknesses. Furthermore, insulator products with low σ (such as 1_200) show very small values at low frequencies and very large values at high frequencies. For open-pore insulator products with large airflow resistivity (such as 4_200), the difference between low and high frequencies is not so large but the curve is flatter. These findings agree with a previous experimental study [10].

When the thickness increases, the performance of porous materials at middle and low frequencies improves while the high frequency performance remains the same. This agrees both with previous experimental findings [10] and with the theory [25]. Theory suggests that an absorption material can only reach it maximum performance, when the material thickness d becomes larger than $\lambda_m/4$, where λ_m is the wavelength of sound in the material. The corresponding limit frequencies are 1715 Hz, 857 Hz, and 428 Hz for thicknesses 50, 100, and 200 mm. It is quite clear in Fig. 7, that the plateaus are reached approximately at these frequencies.

The exception among the porous insulator products is cellulose which shows a weak dip at high frequencies. The dip frequency gets lower with increasing thickness. We could not explain this exception and further research is needed to confirm this finding.

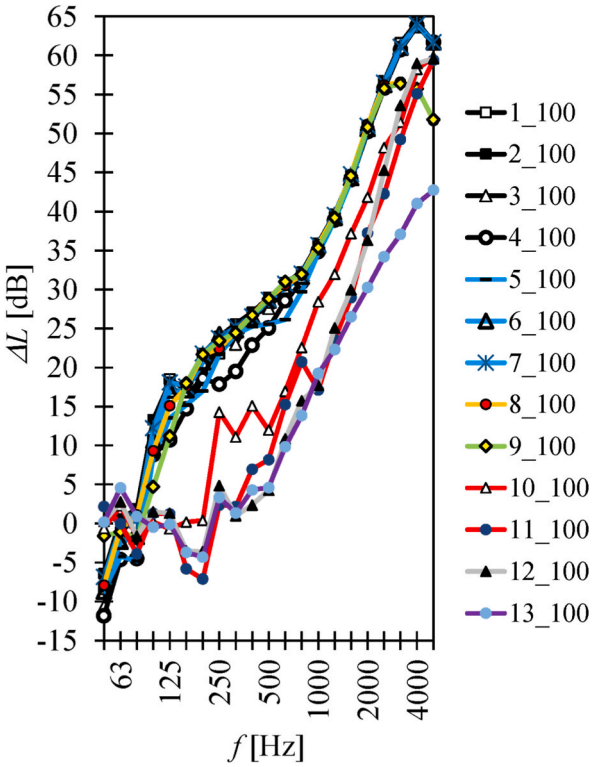

Fig. 10. Reduction of impact sound pressure level, ΔL, as a function of frequency, f, in a floating floor setup for the 13 insulator types with thickness $d = 100$ mm. Numerical values are shown in Table S5 (Supplementary data).

Table 3
Pearson's correlation coefficient between the physical quantities determined for 13 different insulator types with 100 mm thickness. Values denoted by *** indicate that the association is statistically highly significant ($p < 0.001$). Values denoted by ** indicate that the association is statistically significant ($p < 0.01$). Values denoted by * indicate that the association is statistically significant ($p < 0.05$) but the association is weak.

(alignment by comma)

	ρ	λ	α_M	s'	ΔL_w	R_{w1}	R_{w2}	σ
ρ	1	−0.00	−0.03	0.51	−0.07	0.74**	−0.02	−0.24
Λ		1	0.67*	0.02	0.64*	−0.36	0.68*	−0.89***
α_M			1	−0.45	0.99**	−0.46	0.99**	−0.76**
s'				1	−0.52a	0.66*	−0.47	−0.08
ΔL_w					1	−0.49	0.99***	−0.74**
R_{w1}						1	−0.44	0.12
R_{w2}							1	−0.78**
Σ								1

All closed-pore insulator products (10–13) showed strong resonant behavior: absorption is low at most frequencies except at a specific frequency, where a very high absorption is reached. It is also questionable why the absorption peak occurs at the same frequency range independent of insulator product, since these products have different microscopic structures. We are not completely sure about the origin of the absorption peak. Resonance behavior is normal for panel absorbers and Helmholz resonators which have established theories [25]. The latter type requires that the insulator product involves an impervious surface which is perforated and there is a backing volume behind these perforations. However, this is not the case: the pores are microscopic and continue throughout the material. Panel absorber requires that the sample forms a mass-spring-mass system. Since the closed-pore insulator products are homogenic and almost impervious due to extremely large airflow resistivity, it is feasible to expect that a tiny air cavity, which inevitably remains between these hard insulator products and rigid steel backing, could act as a spring and the entire insulator product acts the mass. We attempted to avoid such a gap by manually compressing the sample against the rigid steel backing in the impedance tube. The resonance frequency of such a system is approximated by

$$f_0 = \frac{62}{\sqrt{m' d_c}} \tag{14}$$

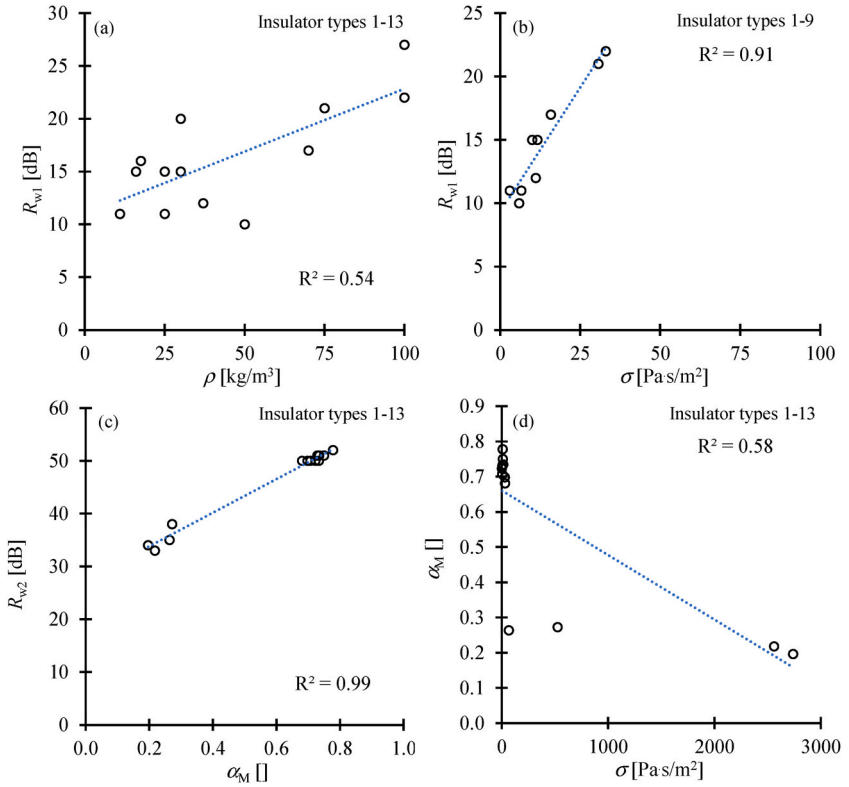

Fig. 11. Examples of some relevant statistically significant associations between physical quantities. (a) Weighted sound reduction index of bare insulator product, R_{w1}, versus density ρ. (b) R_{w1} versus specific flow resistance, σ. (c) Weighted sound reduction index of encapsulated insulator product, R_{w2}, versus mean absorption coefficient, α_M. (d) α_M versus σ.

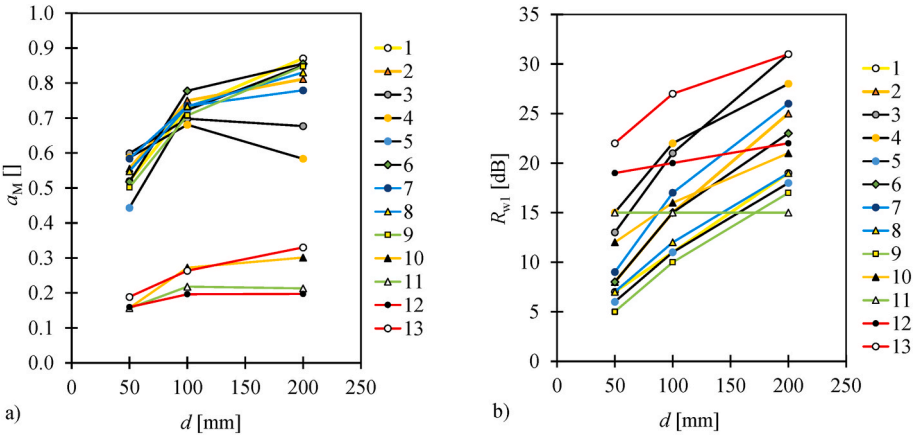

Fig. 12. a) Mean absorption coefficient within 100–3150 Hz, a_M, as a function of thickness, d, for insulator types 1–13. b) Weighted sound reduction index, R_{w1}, as a function of thickness, d, for insulator types 1–13.

where m' [kg/m^2] is the surface mass and d_c [m] is the thickness of the cavity behind the sample. For example, insulator product 10_50 has m' = 0.9 kg/m^2. An air cavity of $d_c = 2$ mm would produce the observed value of $f_0 = 1250$ Hz. This explanation model is supported by the fact that the resonance frequency reduces with increasing thickness. Furthermore, the order of the resonance frequencies slightly varies between thicknesses, which is caused by the fact that the manual compression does not always lead to exactly same d_c for different insulator products. If this explanation is true, the resonance peak does not describe the inherent properties of insulator types 10–13. That is, the actual sound absorption coefficient of closed-pore materials could be lower than reported. In the future, such materials could be tested by using a thick layer of adhesive material (such as vaseline) behind the test sample to avoid the formation of air cavity.

4.3. Sound reduction index of bare insulator products

Most of the insulator types showed a monotonic increase of sound reduction index in bare installation, R_1, as a function of frequency at and above 80 Hz (Fig. 8). Exceptions were the insulator types 10–12 which showed reductions of R_1 at high frequencies at all three thicknesses. The same insulator types appeared to have also smaller sound absorption coefficient than the others. Fig. 11a indicates the association between R_{w1} and ρ (density) among the 13 insulator types. R_{w1} is strongly dependent on density. This agrees with the prediction model of Ref. [15], which is developed for wrappings and linings of porous materials. However, the density explains only 54% of variation: 46% is explained by other factors. Coefficient of determination, R^2, was almost the same (0.59) if the analysis was limited to open-pore insulator types 1–9. Future research is needed to systematically analyze how accurately the model of Ref. [15] predicts the observed R_1 values.

R_1 usually increases with increasing thickness (Fig. 12b) because the surface mass increases. There are two exceptions to that: R_{w1} of insulator types 11 and 12 did not increase with thickness as found for all other insulator types (Fig. 12). These insulator types behaved like impervious building boards Since they had a clear coincidence frequency, which reduces with increasing thickness. Because the coincidence frequency for the smallest thickness is relatively high (2000 Hz and 5000 Hz for insulator types 11 and 12, respectively), the adverse influence of the coincidence dip on R_{w1} is smaller than with the largest thickness (1000 Hz and 1250 Hz for insulator types 11 and 12, respectively) where the whole coincidence dip is located within the range 100–3150 Hz, where R_w is determined.

It is extraordinary that insulator product 3_200 (15 kg/m^2) reached $R_1 > 70$ dB at 4000–5000 Hz, which is approximately the same as measured for a 180-mm thick steel-reinforced concrete wall weighing 30 times more (450 kg/m^2) [26]. Mass law [14,24] states that for single-layer boards, the SRI depends on surface mass, m' [kg/m^2] and frequency, f [Hz], according to

$$R = 20 \cdot \log_{10}(m' \cdot f) - 48 \tag{15}$$

The mass law suggests that the SRI of insulator product 3_200 varies between 10 dB (50 Hz) and 50 dB (5000 Hz). Obviously, open-pore insulator products, such as 3_200, did not follow the mass law. Instead, R_1 seemed to depend at high frequencies linearly on thickness. This finding supports the theory of Ref. [15], according to whom the SRI at high frequencies depends on thickness d, and sound absorption coefficient, α. According to Ref. [15], the SRI in porous materials is not only based on surface mass but also on friction caused by the dense packed fibers, where the sound energy transforms into thermal energy. Mass law applies for massive constructions lacking such fibers – mass law is purely based on reflection (impedance mismatch between air and construction) and energy transformation processes do not take place.

However, the R_1 values of thermal insulators were small at frequencies below 500 Hz. For example, the SRI of 180-mm concrete is around 40–55 dB within 50–500 Hz. The R_{w1} values were never above 31 dB. Therefore, bare isolators cannot compete with impervious wall constructions which nearly always perform better than $R_{w1} = 31$ dB.

The R_1 values at 50 and 63 Hz are almost independent of insulator type. This finding is most probably caused by methodological reasons: it is known that the SRI measurement according to ISO 10140–2 [16] is sensitive to modal coupling of the measurement rooms at low frequencies. Therefore, the R_1 values at 50 and 63 Hz may be caused by these methodological reasons rather than material properties.

4.4. Sound reduction index of encapsulated insulator types

The SRI of encapsulated insulator products (see R_2 of Fig. 9) was only tested for 100 mm thickness, since this thickness was available for all insulator types. The curves follow the frequency behavior obtained in a previous experimental study involving a large setup of double constructions [6]. First, there is a strong dip at 80 Hz. This is caused by the mass-air-mass resonance frequency, f_{mam}, of the double construction. It is caused by two boards and air spring. It is calculated by [24]

$$f_{mam} = 80\sqrt{\frac{(m'_1 + m'_2)}{d m'_1 m'_2}} \tag{16}$$

where d [m] is the cavity thickness and m'_1 and m'_2 [kg/m^2] are the surface masses of boards 1 (6.0 kg/m^2) and 2 (9.9 kg/m^2), respectively. In our case, Eq. (16) gives $f_{mam} = 131$ Hz. Fig. 9 suggests that the dip locates already at 80 Hz. Anyhow, below f_{mam}, the behavior is mainly due to modal coupling and differences between insulator types can be neglected. Above f_{mam}, SRI is known to increase rapidly with increasing frequency [24]. The steepness depends on sound absorption coefficient of the cavity. Since there are no mechanical connections (i.e., studs or rails) between the boards, increment of SRI continues up to 1600–2000 Hz.

The dip at 2500–3150 Hz is caused by the coincidence frequencies of veneer and gypsum, not because of the properties of the insulator. To prove this, we also showed the SRI of bare veneer and gypsum boards in Fig. 9.

Open-pore and closed-pore insulator types are clearly divided into two groups. Double construction with open-pore insulator types in the cavity performs extremely well compared to closed-pore insulator types: R_2 of open-pore insulator types reaches 70 dB at high frequencies while the SRI of closed-pore insulator types remains below 60 dB. The open-pore insulator types have higher sound absorption coefficient. This property efficiently prevents the reverberation in the cavity (due to transformation of sound energy in thermal energy in fibers) and this phenomenon is reflected as an increased SRI.

We also tested the SRI of the double construction with an empty cavity so that the cavity was filled only with air (Air_100). It is outstanding that closed-pore insulator types yielded almost the same R_2 as with an empty cavity. No increment of R_2 at any frequency is observed for closed-pore insulator types in comparison to empty cavity. This supports the analysis above that the absorption peaks in

Fig. 7 could be caused by methodological reasons (panel resonator) rather than actual material properties. Fig. 9 confirms our expectation of Sec. 4.2 that the sound absorption coefficient of closed-pore insulator type is negligible. The reverberation inside the cavity is strong as it is when the cavity is empty (filled with air).

Insulator types 11–13 showed a weak dip at 315–400 Hz. This is probably caused by the fact that the veneer and gypsum boards caused a mechanical compression perpendicular to the insulator face. Because the acoustic construction resembles then a sandwich construction, a dilatation resonance according to Eq. (12) occurs [11]. The mechanical compression occurred although we attempted to avoid any compression. Therefore, these three insulator types may be sensitive to similar effects also in practical constructions.

4.5. Strengths and weaknesses

Our study gives the broadest understanding so far about the acoustic properties of commercial thermal insulators since we studied 13 insulator types having different density and raw material. Furthermore, three different thicknesses were included from every insulator type so that 39 different insulator products were tested. Since the insulator products were collected from the North European market, it is possible that some thermal insulator types which are usual in other continents are not represented. Furthermore, open-pore insulators were better represented than closed-pore insulators. It is possible that certain analyses would result in different outcomes if the weighting between these two insulator types were different. Therefore, future research should focus on extending the number of current insulator types. Despite of this limitation, our work gives very useful information that benefits both further research and practical engineering.

Our study is among the first studies to show the dramatic airborne sound insulation differences of thermal insulators in encapsulated condition. Porous insulators perform acoustically much better than non-porous insulators. If the building locates in a noisy area, the choice of thermal insulator affects the environmental noise level indoors. An optimized building envelope considers both thermal and acoustic factors: a material which has high thermal insulation is not necessarily optimal in acoustic insulation. Therefore, our study has significant applications both in building engineering and future development of sustainable thermal insulators.

Our study is one of the few studies publishing experimental data about the sound insulation performance of bare thermal insulators (R_1). The knowledge is extremely useful for designing wrappings and linings, where the thermal insulator remains visible.

5. Conclusions

The acoustic properties of thirteen commercially available thermal insulator types were investigated using three thicknesses: 50 mm, 100 mm, and 200 mm. Thermal insulators' acoustic properties varied significantly (Appendix). Lower thermal conductivity was associated with worse acoustic performance of two primary acoustic quantities: reduction of impact sound insulation in a floating floor setup, ΔL_w, and sound reduction index of encapsulated insulator, R_{w2}. That is, better thermal insulation may lead to worse thermal insulation and sound reduction index. Open-pore insulator types usually carried better acoustic performance than closed-pore insulator types. Because of the drastic differences between insulator types, and the abovementioned undesirable associations, special attention should be paid on the selection of thermal insulator, when the insulated target (e.g., wall, floor, door, roof, duct wrapping, machine, vehicle envelope) has acoustic requirements. Most of the acoustic data reported in this study was not available in the product specifications. Insulator manufacturers should consider to better declare the acoustic properties of insulator products, because this knowledge is needed in the acoustic design of building constructions and other applications where thermal insulators are used.

Author statement

Conceptualization: VH; Data curation: VH, PS, RA. Formal analysis: VH. Funding acquisition: VH; Investigation: RA, PS, JH. Methodology: VH, PS, JH, RA. Project administration: VH. Resources: VH. Software: VH. Supervision: VH. Validation: VH. Visualization: VH, PS, JH. Writing - original draft; VH, PS. Writing - review & editing: VH.

Declaration of competing interest

The authors declare that they have no known competing financial interests or personal relationships that could have appeared to influence the work reported in this paper.

Acknowledgements

The project was funded by Paroc Group Ltd./Owens Corning.

Appendix A. Supplementary data

Supplementary data to this article can be found online at https://doi.org/10.1016/j.jobe.2022.104588.

Appendix

Table
The value range of the studied quantities for the 13 insulator types with 100 mm thickness.

	λ [W/mK]	m' [kg/m^2]	α_M [ ]	s' [MN/m^3]	ΔL_w [dB]	R_{w1} [dB]	R_{w2} [dB]	σ [kPa·s/m^2]
Minimum	0.020	1.1	0.20	1.5	15	10	33	3.0
Maximum	0.044	10	0.78	730	36	27	52	2700

λ - thermal conductivity.
m' - surface mass.
α_M - mean absorption coefficient within 100-3150 Hz.
s' - dynamic stiffness per unit area.
ΔL_w - weighted reduction of impact sound pressure level in a floating floor.
R_{w1} - weighted sound reduction index of bare insulator.
R_{w2} - weighted sound reduction index of encapsulated insulator (between two boards).
σ - airflow resistivity.

References

[1] L. Aditya, T.M.I. Mahliaa, B. Rismanchi, H.M. Ng, M.H. Hasan, H.S.C. Metselaar, O. Muraza, H.B. Aditiya, A review on insulation materials for energy conservation in buildings, Renew. Sustain. Energy Rev. 73 (2017) 1352–1365.
[2] A.M. Papadopoulos, State of the art in thermal insulation materials and aims for future developments, Energy Build. 37 (2005) 77–86.
[3] M. Caniato, A. Marzi, S. Monteiro da Silva, A. Gasparella, A review of the thermal and acoustic properties of materials for timber building construction, J. Build. Eng. 43 (2021), 103066.
[4] WHO, Environmental Noise Guidelines for the European Region, World Health Organization. Regional Office for Europe, Copenhagen, Denmark, 2018.
[5] Finnish Government, in: Government Decree 993/1992 about the Regulated Noise Levels (Valtioneuvoston Päätös Melutason Ohjearvoista), 29th October, 1992. Helsinki, Finland (In Finnish). Available at: https://www.finlex.fi/fi/laki/alkup/1992/19920993.
[6] V. Hongisto, M. Lindgren, R. Helenius, Sound insulation of double walls - an experimental parametric study, Acta Acustica united Acustica 88 (2002) 904–923.
[7] D. Urbán, P. Zat'ko, N.B. Roozen, H. Muellner, C. Glorieux, Influence of the dynamic stiffness of external thermal insulation on the sound insulation of walls, Proc. Euronoise (2018) 1521–1524, 27–31 May, Hersonissos, Crete, Greece.
[8] E. Moretti, E. Belloni, F. Agosti, Innovative mineral fiber insulation panels for buildings: thermal and acoustic characterization, Appl. Energy 169 (2016) 421–432.
[9] U. Berardi, G. Iannace, Acoustic characterization of natural fibers for sound absorption applications, Build. Environ. 94 (2015) 840–852.
[10] D. Oliva, V. Hongisto, Sound absorption of porous materials - accuracy of existing prediction methods, Appl. Acoust. 74 (2013) 1473–1479.
[11] V. Hongisto, A case study of flanking transmission through double structures, Appl. Acoust. 62 (5) (2001) 589–599.
[12] V. Hongisto, P. Virjonen, H. Maula, P. Saarinen, J. Radun, Impact sound insulation of floating floors: a psychoacoustic experiment linking standard objective rating and subjective perception, Build. Environ. 184 107225 (2020) 12.
[13] DIN, DIN 4109-34/A1 Sound Insulation in Buildings – Part 34: Data for Verification of Sound Insulation (Component Catalogue) – Additional Layers Fixed to Solid Structural Elements, 2019. Amendment A1 (In German).
[14] J.H. Rindel, Sound Insulation in Buildings, CRC Press, Taylor & Francis Group, Boca Raton. Florida, USA, 2018.
[15] T.J. Schultz, Ch. 15: wrappings, enclosures, and duct linings, in: L.L. Beranek (Ed.), Noise and Vibration Control, McGraw-Hill Book Company, New York, USA, 1971, pp. 476–511.
[16] ISO, ISO 10140-2 Acoustics — Laboratory Measurement of Sound Insulation of Building Elements — Part 2: Measurement of Airborne Sound Insulation, 2010.
[17] ISO, ISO 717-1. Acoustics — Rating of Sound Insulation in Buildings and of Building Elements — Part 1: Airborne Sound Insulation, 2020.
[18] ISO, ISO 3382-2 Acoustics — Measurement of Room Acoustic Parameters — Part 2: Reverberation Time in Ordinary Rooms, 2008.
[19] ISO, ISO 10534–2 Acoustics — Determination of Sound Absorption Coefficient and Impedance in Impedance Tubes — Part 2: Transfer-Function Method, 1998.
[20] ISO, ISO 9053-1 Acoustics — Determination of Airflow Resistance — Part 1: Static Airflow Method, 2018.
[21] ISO, ISO 9052-1 Acoustics — Determination of Dynamic Stiffness — Part 1: Materials Used under Floating Floors in Dwellings, 1989.
[22] ISO, ISO 10140-3 Acoustics — Laboratory Measurement of Sound Insulation of Building Elements — Part 2: Measurement of Impact Sound Insulation, 2010.
[23] ISO, ISO 717-2 Acoustics. Rating of Sound Insulation in Buildings and of Building Elements. Part 2: Impact Sound Insulation, 2020.
[24] V. Hongisto, Sound insulation of doors - Part 1: prediction models for structural and leak transmission, J. Sound Vib. 230 (1) (2000) 133–148.
[25] T. Cox, D'Antonio, P. Acoustic Absorbers and Diffusers. Theory, Design and Application, Spon Press, Oxon, UK, 2004.
[26] V. Hongisto, D. Oliva, J. Keränen, Subjective and objective rating of airborne sound insulation – living sounds, Acta Acustica united Acustica 100 (2014) 848–863.